Estimation of stopped protons at energies relevant for a beam energy scan at the BNL Relativistic Heavy Ion Collider

Dhananjaya Thakur,[1] Sunil Jakhar,[1] Prakhar Garg,[1,2] and Raghunath Sahoo[1,*]

[1]*Discipline of Physics, School of Basic Sciences, Indian Institute of Technology Indore, Indore 453552, India*

[2]*Department of Physics and Astronomy, Stony Brook University, SUNY, Stony Brook, New York 11794-3800, USA*

(Received 14 November 2016; revised manuscript received 1 February 2017; published 10 April 2017)

The recent net-proton fluctuation results of the STAR (Solenoidal Tracker At RHIC) experiment from the beam energy scan (BES) program at the BNL Relativistic Heavy Ion Collider (RHIC) have drawn much attention to exploring the QCD critical point and the nature of deconfinement phase transition. There has been much speculation that the nonmonotonic behavior of $\kappa\sigma^2$ of the produced protons around $\sqrt{s_{NN}} = 19.6$ GeV in the STAR results may be due to the existence of a QCD critical point. However, the experimentally measured proton distributions contain protons from heavy resonance decays, from baryon stopping, and from direct production processes. These proton distributions are used to estimate the net-proton number fluctuation. Because it is difficult to disentangle the protons from the above-mentioned sources, it is better to devise a method which will account for the directly produced baryons (protons) to study the dynamical fluctuation at different center-of-mass energies. This is because it is assumed that any associated criticality in the system could affect the particle production mechanism and hence the dynamical fluctuation in various conserved numbers. In the present work, we demonstrate a method to estimate the number of stopped protons at RHIC BES energies for central 0–5% Au+Au collisions within STAR acceptance and discuss its implications on the net-proton fluctuation results.

DOI: 10.1103/PhysRevC.95.044903

I. INTRODUCTION

One of the main motivations of studying heavy-ion collisions is to explore the QCD phase diagram of the strong interaction. Quantum chromodynamics predicts a phase transition from a hadron gas (HG) phase to a quark-gluon plasma (QGP) phase by varying the temperature T and/or baryon density μ_B of the system. Lattice QCD calculations indicate a smooth crossover along the temperature axis, while various other models predict a first-order phase transition at high baryon density. The existence of the QCD critical point is thus expected at finite μ_B and T, where the first-order phase transition line ends [1–8]. The search for the QCD critical point is one of the main motivations behind the recent STAR (Solenoidal Tracker At RHIC) net-proton [9], net-charge [10], and PHENIX net-charge [11] measurements at the BNL Relativistic Heavy Ion Collider (RHIC). It is necessary to look into the dynamical behavior of the produced system by considering the observable effects of baryon stopping and initial-state participant fluctuations. To do this, the present work is an effort to quantify the effect of stopped baryons, which are prevalent at lower collision energies around the RHIC Beam Energy Scan (BES), where a possible critical point in the QCD phase diagram is expected to be observed.

The phenomenon of baryon stopping could be used as a direct tool to explore the QCD phase transition and as a probe of the equation of state (EOS) of the system [12]. The reduced curvature obtained from the net-proton rapidity distribution at midrapidity is used as an observable for baryon stopping. As discussed in Ref. [12], the behavior of the midrapidity curvature with $\sqrt{s_{NN}}$ has been studied and a zig-zag type of structure is observed. A three-fluid dynamics (3FD) calculation with hadronic EOS fails to explain the observed structure, whereas 3FD with first-order phase transition from a hadronic phase to a deconfined phase of quark-gluon plasma qualitatively reproduces the structure [12]. Hence, it is argued that the nonmonotonic behavior of baryon stopping is due to a phase transition and is most probably of first order in nature. Theoretical studies based on STAR net-proton fluctuation [9] hint for a phase transition at low $\sqrt{s_{NN}}$ taking inclusive protons, i.e., from both production and stopping. However, as baryon stopping plays a major role at lower collision energies and almost vanishes at higher energies, there seems to be a need to disentangle the contribution of stopped baryons and the produced baryons in order to understand the observed structures and hence the QCD phase diagram.

The conserved number fluctuations are associated with the possible existence of a critical point, which are dynamical in nature. The present work is motivated to re-visit the net-baryon (proton) number fluctuation, which is related to the particle production mechanism. But most of the experimentally measured proton distributions contain the protons from stopping and resonance decays besides those from direct production. Also, it has been studied earlier that the change in the mean of proton distributions (which will be there, after subtracting the stopped protons) will have a large effect on the correlation of the protons and antiprotons, and it can influence the higher moments of net-proton fluctuations [13]. Particularly, at lower center-of-mass energies the stopping contribution is most dominant and it will be interesting to look for the dynamical fluctuations after removing these stopped protons. Various other effects on the conserved number fluctuations have been studied earlier in Refs. [13–18].

In heavy-ion collision experiments, a part of the incident energy of the two colliding nuclei is used for fireball production

*Raghunath.Sahoo@cern.ch

and hence the production of secondary particles. Therefore, the formation of a QGP in relativistic heavy-ion collisions depends on the amount of stopping between the colliding ions, particularly at low center-of-mass energies. Hence, baryon stopping serves as an important tool to understand the particle production mechanism. As the net-baryon number is conserved and rapidity distribution is modified due to rescattering of the particles after the collision, the net-baryon rapidity distribution becomes a useful probe to give information about baryon transport and baryon stopping. Since neutrons are not measured in most heavy-ion experiments, the net-proton rapidity distributions are used to quantify the baryon stopping [19–24].

In the present work, we use the data of net-proton rapidity distributions for the most central Au+Au collisions measured at the BNL Alternating Gradient Synchrotron (AGS) and CERN Super Proton Synchrotron (SPS), and by the BRAHMS experiment at RHIC. We use a two-source function [12] to analyze the net-proton distributions at different center-of-mass energies. It is a combination of two thermal sources with a shift in their rapidities. The same two-source function is used in the present work to calculate the percentage of stopped protons. Afterword, the percentage of stopped protons with $\sqrt{s_{NN}}$ is parametrized and the values at RHIC BES energies are interpolated. Finally, we estimate the contribution of stopped protons in rapidity $|y| < 0.5$ and transverse momenta between 0.4 and 0.8 GeV/c, which are used to measure the protons and antiprotons by the STAR experiment for net-proton fluctuation studies [9].

The paper is organized as follows. In Sec. II, we discuss the method used for the present analysis. It is divided into three subsections: (a) estimation of baryon stopping in $|y| < 0.5$ (Sec. II A), (b) estimation of stopped protons in the STAR transverse momentum (p_T) range (Sec. II B), and (c) contribution of stopped protons in STAR measurements (Sec. II C). We briefly discuss the implications of this work to the net-proton fluctuation results of the STAR experiment at RHIC in Sec. III. Finally in Sec. IV, we summarize our work.

II. METHOD

A. Estimation of baryon stopping in $|y| < 0.5$

Net-proton rapidity distribution of the experimental data is best described by the following function:

$$dN/dy = a[\exp\{-(1/w_s)\cosh(y - y_{\text{c.m.}} - y_s)\} + \exp\{-(1/w_s)\cosh(y - y_{\text{c.m.}} + y_s)\}], \quad (1)$$

where a, y_s, and w_s are the fit parameters of the function and $y_{\text{c.m.}}$ is the center-of-mass rapidity of the colliding nuclei [12]. Equation (1) is the sum of two thermal sources shifted by rapidity $\pm y_s$ from the midrapidity. w_s is the width of the sources and is given by w_s = (temperature)/(transverse mass), with the assumption that there is no spread of collective velocities in the sources with respect to the source rapidities. We have used Eq. (1) to fit the net-proton rapidity distributions to quantify the baryon stopping. Since we are concerned about symmetric collisions, the parameters of the two sources are taken as identical. Parameters y_s and w_s are calculated from the fitted function to the rapidity distribution of the secondary particles.

Baryon stopping is directly measured via the rapidity distribution of net-protons (i.e., the number of protons minus antiprotons). At low energies like those at the AGS, the production of antiprotons is very small so the net-proton distribution is assumed to be the same as the proton distribution and the rapidity distribution peaks at midrapidity [12]. As the collision energy increases, a dip begins to appear at midrapidity ($y \approx 0$) and the peak shifts toward the forward and backward rapidities, due to the production of antiprotons at midrapidity. This indicates that with an increase in the energy, the transparency at midrapidity increases. The rapidity loss of the particle is defined as $y_{\text{loss}} = y_b - y$, where $y_b = \ln(\sqrt{s_{NN}}/m_p)$ is the beam rapidity with m_p the mass of the proton.

Therefore, the net-baryon number at midrapidity is the measure of baryon stopping [19–21]. To quantify the baryon stopping, we used Eq. (1) to fit the data of rapidity distribution for the most central Au+Au collisions at AGS energies (2A, 4A, 8A GeV), and BRAHMS data at RHIC energies (62.4 and 200 GeV). The fitting is performed using the TMinute class available in the ROOT library with χ^2 minimization. This is shown in Fig. 1 along with the fit functions for different energies. Further, these fit functions are used to estimate baryon stopping at the corresponding collision energies.

In the center-of-mass system, the maximum rapidity that an outgoing particle can have after the collision is y_b, which is

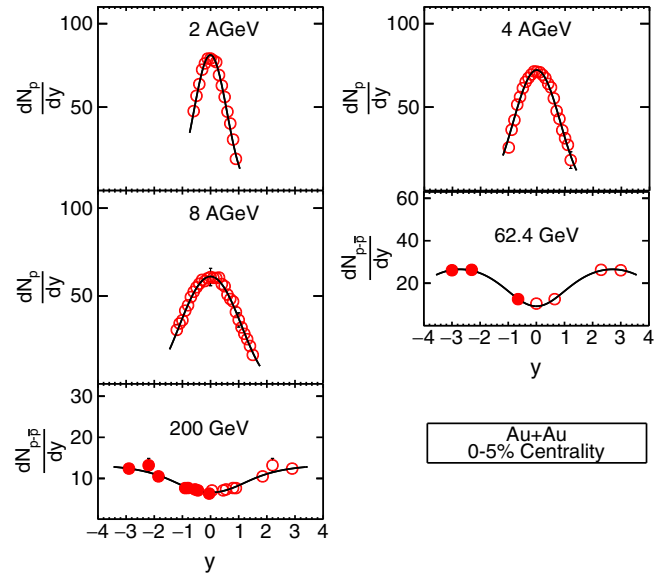

FIG. 1. Rapidity densities of protons at 2A, 4A, and 8A GeV (AGS) and net-proton ($N_p - N_{\bar{p}}$) (for RHIC energies) for central Au+Au collisions in the center-of-mass system. Experimental data are from E802 [25], E877 [26], E917 [27], E866 [28], and RHIC experiments [20,24]. The open circles are experimentally measured data points and the filled circles are the mirror reflections, assuming a symmetry in particle production. Solid lines represent the two-source fit function given by Eq. (1).

TABLE I. Fraction of stopped protons in $|y| < 0.5$ at different energies.

$\sqrt{s_{NN}}$ (GeV)	$E_{\rm lab}$ (GeV/nucleon)	$N^{\rm protons}_{\rm stopped}(\%)$
2.35	2	64.22 ± 0.10
3.04	4	52.16 ± 0.15
4.09	8	44.61 ± 0 .12
62.4		4.57 ± 0.10
200		2.91 ± 0.0

only possible for full transparency. Therefore, by using Eq. (1), the fraction of stopped protons in $|y| < 0.5$ at a particular energy can be calculated as

$$f^{\rm protons}_{\rm stopped} = \frac{\int_{-0.5}^{0.5} \frac{dN}{dy} dy}{\int_{-y_b}^{y_b} \frac{dN}{dy} dy}. \quad (2)$$

Hence, the percentage of stopped protons can be estimated as

$$N^{\rm protons}_{\rm stopped}[\%] = f^{\rm protons}_{\rm stopped} \times 100\%. \quad (3)$$

It should be noted here that $\int_{-y_b}^{y_b} \frac{dN}{dy} dy$ gives the total number of participating protons ($N^B_{\rm part}$) and for the top central Au+Au collisions, $N^B_{\rm part} \approx 158$. The calculated percentages of stopped protons at these energies are shown in Table I.

Thereafter, by converting the laboratory energy to the center-of-mass energy, a study of percentage of stopped protons with $\sqrt{s_{NN}}$ is done. The decreasing behavior of stopped protons ($N^{\rm proton}_{\rm stopped}[\%]$) with $\sqrt{s_{NN}}$ is best described by an exponential function as shown in Fig. 2. Our observations are in line with the earlier study [19]. Hence, a parametric form of the percentage of stopped protons with $\sqrt{s_{NN}}$ is obtained. This is given by $N^{\rm protons}_{\rm stopped}[\%] = A \exp[-B \ln(\sqrt{s_{NN}/s_0})]$, where $\sqrt{s_0}$ is taken to be 1 GeV and the obtained fitting parameters are $A = 118.89 \pm 6.18$ and $B = 0.72 \pm 0.05$. Using this parametrized function, we have interpolated the percentage of stopping at RHIC BES energies in $|y| < 0.5$ for $\sqrt{s_{NN}} =$ 7.7, 11.5, 19.6, 27, 39, 62.4, and 200 GeV. The values are tabulated in Table II.

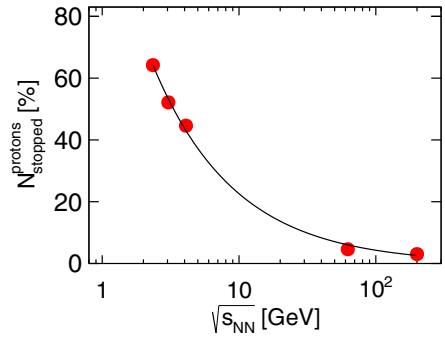

FIG. 2. Percentage of baryon stopping as a function of $\sqrt{s_{NN}}$, fitted with an exponentially decreasing function with energy.

TABLE II. Percentages of stopped protons at different RHIC BES energies in $|y| < 0.5$ acceptance.

$\sqrt{s_{NN}}$ (GeV)	7.7	11.5	19.6	27	39	62.4	200
$N^{\rm protons}_{\rm stopped}$ (%)	27.27	20.43	13.90	11.03	8.46	6.03	2.60
Err$\{N^{\rm protons}_{\rm stopped}\%\}$	1.30	1.34	1.25	1.15	1.03	0.86	0.51

B. Estimation of stopped protons in STAR p_T acceptance

In the previous section, we estimated the percentage of stopped protons in $|y| < 0.5$ at RHIC BES energies. But the STAR experiment measured the protons and antiprotons in $0.4 < p_T < 0.8$ GeV/c to calculate the higher order cumulants of net-proton distributions [9]. After estimating the number of stopped protons at midrapidity, we calculate the same in the STAR p_T acceptance. Here we assume that the stopped protons are uniformly distributed over the whole p_T spectra. To estimate the fraction of the stopped protons in STAR p_T acceptance we have fitted the proton p_T spectra at

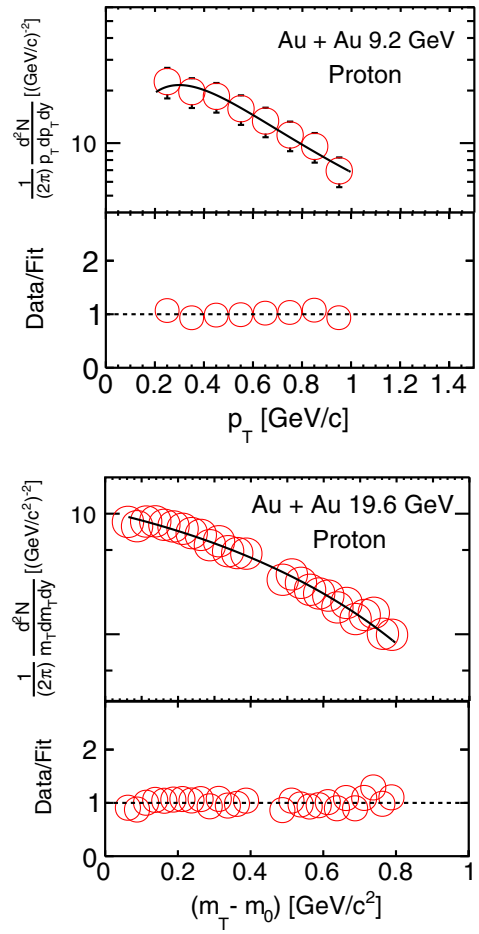

FIG. 3. Invariant yield of protons at $\sqrt{s_{NN}} = 9.2$ [35] and 19.6 [31] GeV for the most central Au+Au collisions. The open circles are the experimental data measured by the STAR Collaboration. The solid lines are the Levy-Tsallis function [29] for $\sqrt{s_{NN}} = 9.2$ and the Tsallis function [30] for $\sqrt{s_{NN}} = 19.6$ GeV. The lower panels show the ratio of data points to their functional values.

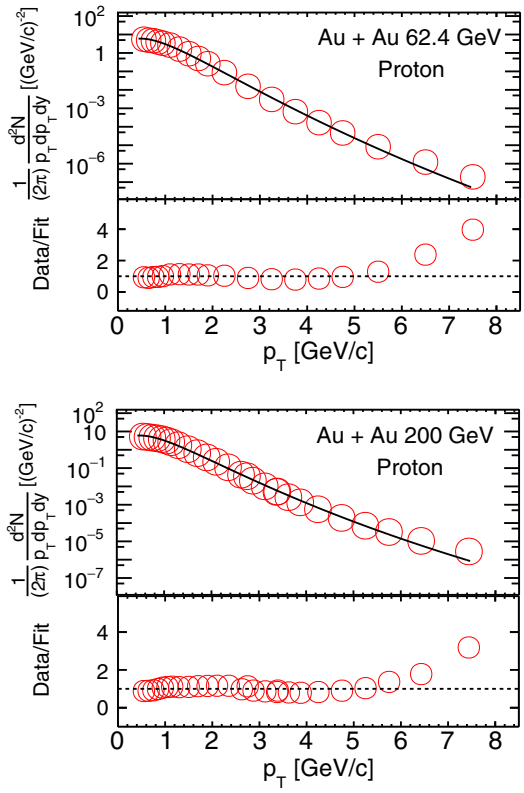

FIG. 4. Invariant yield of protons at 62.4 [32] and 200 [33] GeV for the most central Au+Au collisions. The open circles are the experimental data measured by the STAR Collaboration. The solid lines are the Levy-Tsallis function [29]. The lower panels show the ratio of data points to their functional values.

different available BES energies. The fitting is performed with a Levy-Tsallis function, which is given by Eq. (11) of Ref. [29] for $\sqrt{s_{NN}} = 9.2$, 62.4, and 200 GeV. Similarly, for $\sqrt{s_{NN}} =$ 19.6 GeV, the Tsallis distribution function, as given by Eq. (6) of Ref. [30] is used. The fitting results of STAR proton data are shown in Figs. 3 and 4. The ratios in the lower panels of Figs. 3 and 4 suggest that the fit functions used describe the experimentally measured proton spectra very well for all center-of-mass energies. We integrate the fitted functions at a

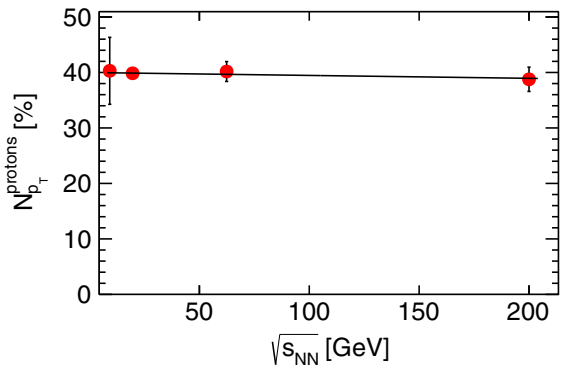

FIG. 5. Percentage of protons in $0.4 < p_T < 0.8$ GeV/c as a function of $\sqrt{s_{NN}}$ are well described by a first-order polynomial.

TABLE III. Percentages of protons obtained from p_T spectra at different BES energies in STAR p_T acceptance.

$\sqrt{s_{NN}}$ (GeV)	7.7	11.5	19.6	27	39	62.4	200
$N^{protons}_{p_T}$(%)	39.95	39.93	39.88	39.84	39.79	39.66	38.94
Err{$N^{protons}_{p_T}$%}	0.60	0.58	0.54	0.52	0.52	0.63	2.11

particular energy from $p_T = 0.0$ to $p_T = \infty$ and $p_T = 0.4$ to 0.8 (GeV/c). Thus the total number of protons in the whole p_T range and the number of protons in $0.4 < p_T < 0.8$ GeV/c are calculated.

The fraction of protons falling in $0.4 < p_T < 0.8$ GeV/c region is estimated as

$$f^{protons}_{p_T} = \frac{N^{protons}(0.4 < p_T < 0.8)}{N^{protons}(\text{full } p_T)}. \quad (4)$$

Hence, the percentage of protons in STAR p_T acceptance is given by

$$N^{protons}_{p_T}[\%] = f^{protons}_{p_T} \times 100\%. \quad (5)$$

Using Eq. (5), one can estimate the fraction of stopped protons contributing in STAR p_T acceptance. To calculate the percentage in the RHIC BES energies, we have parametrized these numbers with $\sqrt{s_{NN}}$ by first-order polynomials as shown in Fig. 5. Then the contributions at different BES energies are interpolated. The extracted values are tabulated in Table III.

C. Contribution of stopped protons in STAR measurements

In the top central Au+Au collisions, around 158 protons participate in each collision. We have already estimated the percentage of number of protons in Table II in $|y| < 0.5$ for full p_T coverage and in Table III for $0.4 < p_T < 0.8$ GeV/c. Therefore, one can easily calculate the effect of both to estimate the total stopped protons in STAR acceptance. This is given by

$$N^{protons}_{stopped}(\text{STAR}) = 158 \times N^{protons}_{stopped}\% \times N^{protons}_{p_T}\%, \quad (6)$$

where $N^{protons}_{stopped}$(STAR) is the total contribution of stopped protons in STAR acceptance. In Table IV we enlist the total number of stopped protons at BES energies in STAR acceptance.

Figure 6 shows the energy-dependent behavior of the stopped protons, which is consistent with the fact that stopping is more at lower energies than at higher energies.

It is interesting to note that after subtracting the stopped protons from the mean of STAR proton distributions [9], the

TABLE IV. Number of stopped protons at different RHIC BES energies in STAR acceptance.

$\sqrt{s_{NN}}$ (GeV)	7.7	11.5	19.6	27	39	62.4	200
$N^{protons}_{stopped}$(STAR)	17.21	12.89	8.76	6.94	5.32	3.78	1.6
Err{$N^{protons}_{stopped}$(STAR)}	0.86	0.86	0.80	0.73	0.65	0.54	0.33

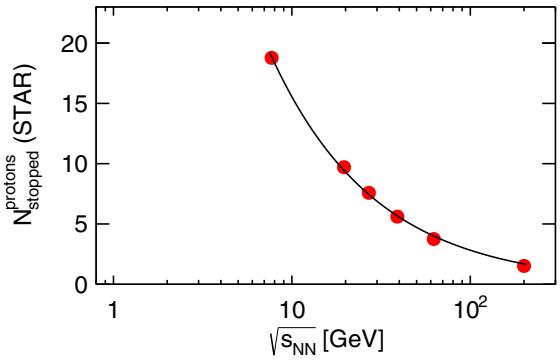

FIG. 6. Mean number of protons from baryon stopping in STAR acceptance as a function of $\sqrt{s_{NN}}$, showing an exponential decrease with energy.

remaining produced protons are consistent with the antiprotons measured by the STAR experiment. This can be seen from Table V. There is a small discrepancy between these two numbers at 7.7 and 11.5 GeV measurements. This may be due to the larger uncertainties in the experimental measurement of the protons.

III. EXPERIMENTAL IMPLICATIONS

The discussed methodology would lead to the estimation of the number of stopped protons that could improve the understanding of dynamical fluctuations. Particularly, the $\kappa\sigma^2$ variable of the produced protons *only* will be useful to study the criticality in the QCD phase diagram. Because it is not possible to tag a proton as coming from stopping or from production in the experimental data, the correction for the stopped protons to the net-proton multiplicity distribution cannot be applied to the experimental measurement. The exact distribution of stopped protons on an event-by-event basis is not known and hence it is difficult to subtract the contribution of stopped protons to the inclusive proton distribution, which needs further investigation. Therefore, it is suggested that while quoting the fluctuation results from net-proton multiplicity distribution, a systematic uncertainty may be added by using the Monte Carlo simulations and the results of this study to quantify the effect of stopping on the fluctuations in their respective acceptance. This proposed analysis bears values in the low-energy BES program of RHIC, where a search for the critical point and the associated criticality becomes prudently viable.

TABLE V. Columns (a) $\sqrt{s_{NN}}$ (in GeV) at which the analysis is performed, (b) mean number of protons obtained from baryon stopping in STAR acceptance, (c) mean number of protons measured by STAR experiment [34], (d) Diff. $=[N^{protons}_{STAR}\text{-}N^{protons}_{stopped}(STAR)]$, and (e) mean number of antiprotons measured by STAR experiment.

(a) $\sqrt{s_{NN}}$	(b) $N^{protons}_{stopped}$(STAR)	(c) $N^{protons}_{STAR}$	(d) Diff.	(e) $N^{antiprotons}_{STAR}$
7.7	17.21 ± 0.86	18.92 ± 0.01	1.71 ± 0.86	0.165
11.5	12.89 ± 0.86	15.00 ± 0.01	2.10 ± 0.86	0.49
19.6	9.73 ± 0.80	11.37 ± 0.00	1.63 ± 0.80	1.15
27.0	7.61 ± 0.73	9.39 ± 0.00	1.78 ± 0.73	1.65
39.0	5.78 ± 0.65	8.22 ± 0.00	2.44 ± 0.65	2.38
62.4	3.78 ± 0.54	7.25 ± 0.00	3.47 ± 0.54	3.14
200	1.54 ± 0.33	5.664 ± 0.00	4.12 ± 0.33	4.11

IV. SUMMARY

In the present work, we use the data of net-proton rapidity distributions for the most central Au+Au collisions measured by different experiments. Further, we use a two-source function [12] to analyze the net-proton distributions and to estimate the percentage of stopped protons at different center-of-mass energies. Then the percentage of stopped protons is interpolated at RHIC BES energies. Afterword, using invariant transverse momentum spectra we estimate the fraction of the number of protons contributing in STAR acceptance. Finally, using these two numbers, we estimate the contribution of stopped protons in $|y| < 0.5$ and transverse momentum between 0.4 and 0.8 GeV/c, which is used to measure the protons and antiprotons by STAR experiment for net-proton fluctuation studies [9]. The critical point of the QCD phase diagram is expected to show large dynamical fluctuations in the produced conserved charges. Therefore, it will be exciting to see these results after removing the contributions of stopped protons, which have significant contributions, particularly at lower collision energies.

ACKNOWLEDGMENTS

The authors gratefully acknowledge discussions with Prof. B. K. Nandi and Dr. Dipak K. Mishra, and thank Dr. Sudipan De for careful reading of the manuscript. D.T. acknowledges financial support from the University Grants Commission (UGC), New Delhi, Government of India.

[1] M. A. Stephanov, K. Rajagopal, and E. V. Shuryak, Phys. Rev. Lett. **81**, 4816 (1998).
[2] M. G. Alford, K. Rajagopal, and F. Wilczek, Phys. Lett. B **422**, 247 (1998).
[3] M. A. Stephanov, Phys. Rev. Lett. **76**, 4472 (1996).
[4] Y. Aoki, G. Endrodi, Z. Fodor, S. D. Katz, and K. K. Szabo, Nature **443**, 675 (2006).
[5] K. Fukushima and T. Hatsuda, Rept. Prog. Phys. **74**, 014001 (2011).
[6] M. A. Stephanov, Prog. Theor. Phys. Suppl. **153**, 139 (2004); Int. J. Mod. Phys. A **20**, 4387 (2005).
[7] Z. Fodor and S. D. Katz, J. High Energy Phys. 04 (2004) 050.
[8] M. A. Stephanov, K. Rajagopal, and E. V. Shuryak, Phys. Rev. D **60**, 114028 (1999).

[9] L. Adamczyk *et al.* (STAR Collaboration), Phys. Rev. Lett. **112**, 032302 (2014).
[10] L. Adamczyk *et al.* (STAR Collaboration), Phys. Rev. Lett. **113**, 092301 (2014).
[11] A. Adare *et al.* (PHENIX Collaboration), Phys. Rev. C **93**, 011901 (2016).
[12] Y. B. Ivanov, Phys. Lett. B **690**, 358 (2010).
[13] D. K. Mishra, P. Garg, and P. K. Netrakanti, Phys. Rev. C **93**, 024918 (2016).
[14] D. K. Mishra, P. Garg, P. K. Netrakanti, and A. K. Mohanty, Phys. Rev. C **94**, 014905 (2016).
[15] D. K. Mishra, P. Garg, P. K. Netrakanti, and A. K. Mohanty, J. Phys. G **42**, 105105 (2015).
[16] P. Garg, D. K. Mishra, P. K. Netrakanti, B. Mohanty, A. K. Mohanty, B. K. Singh, and N. Xu, Phys. Lett. B **726**, 691 (2013).
[17] P. Garg, D. K. Mishra, P. K. Netrakanti, A. K. Mohanty, and B. Mohanty, J. Phys. G **40**, 055103 (2013).
[18] P. Garg, D. K. Mishra, P. K. Netrakanti, and A. K. Mohanty, Eur. Phys. J. A **52**, 27 (2016).
[19] S. Q. Feng and Y. Zhong, Phys. Rev. C **83**, 034908 (2011).
[20] I. G. Bearden *et al.* (BRAHMS Collaboration), Phys. Rev. Lett. **93**, 102301 (2004).
[21] F. Videbaek, J. Phys. Conf. Ser. **50**, 134 (2006).
[22] F. C. Zhou, Z. B. Yin, and D. C. Zhou, Chin. Phys. Lett. **27**, 052503 (2010).
[23] S. Li and S. Q. Feng, Chin. Phys. C **36**, 136 (2012).
[24] I. C. Arsene *et al.* (BRAHMS Collaboration), Phys. Lett. B **677**, 267 (2009).
[25] L. Ahle *et al.* (E802 Collaboration), Phys. Rev. C **60**, 064901 (1999).
[26] J. Barrette *et al.* (E877 Collaboration), Phys. Rev. C **62**, 024901 (2000).
[27] B. B. Back *et al.* (E917 Collaboration), Phys. Rev. Lett. **86**, 1970 (2001).
[28] J. Stachel, Nucl. Phys. A **654**, C119 (1999).
[29] B. I. Abelev *et al.* (STAR Collaboration), Phys. Rev. C **75**, 064901 (2007).
[30] D. Thakur, S. Tripathy, P. Garg, R. Sahoo, and J. Cleymans, Adv. High Energy Phys. **2016**, 4149352 (2016).
[31] R. Picha, Ph.D. thesis, University of California, Davis, 2005 (unpublished).
[32] B. I. Abelev *et al.* (STAR Collaboration), Phys. Lett. B **655**, 104 (2007).
[33] B. I. Abelev *et al.* (STAR Collaboration), Phys. Rev. Lett. **97**, 152301 (2006).
[34] Cumulants of proton and antiproton distribution measured by STAR experiment: https://drupal.star.bnl.gov/STAR/files/starpublications/205/data.html.
[35] B. I. Abelev *et al.* (STAR Collaboration), Phys. Rev. C **81**, 024911 (2010).